Chapter

Mathematical Modeling and Simulation of Development of the Fires in Confined Spaces

Ivan Antonov, Rositsa Velichkova, Svetlin Antonov and Kamen Grozdanov

Abstract

The mathematical models of fire distribution in a confined space–in underground garages and in buildings—are described. Integral and computational fluid mechanics methods are used. The chapter presents the results of a fire simulation using the software Fluent. It uses Reynolds-type turbulence models of the Fire Dynamic Simulation or PyroSim graphical interface with a solution model describing a turbulence. For both cases, the pictures of the spread of fire and smoke over time in an atrium of an administrative building and a five-story building of the TUS were presented.

Keywords: fire simulation, FDS, garages, buildings, numerical simulation

1. Introduction

Mathematical modeling and numerical simulations of fires are an essential decisive part of the solution of important problems related to fire safety, analysis of the development of fires in the investigation of their consequences. The methods that are used must have the necessary accuracy and reliability, as close as possible to the physical picture of the processes.

The actual fire, as it is known, is an uncontrollable combustion process, complex enough and difficult for mathematical interpretation. This is due to its nonstationarity and three-dimensionality, which complicate the modeling of the heat and mass transfer processes observed in them. In the case of fires indoors of underground garages, buildings, and rooms, the development of the fire is accompanied by a change in the chronicle composition and parameters of the combustion products.

This chapter gives two different approaches in dealing with their complexity and implementation of solving the problem. On the other hand, an integrated, relatively simplified technical solution of a new system for preventing the spread of fires in underground garages is given, which is described in details in the chapter.

The second part deals with the basic mathematical apparatus used in CFD-Fluent and FDS software. The results of two fire simulations made by the authors through Fluent and FDS using the PyroSim GUI are presented [1, 2].

2. Fire extinguishing system in large underground garages: integral methods for investigation

In the present part, a simple method (from a technological point of view) is offered for solution of the complex problem. It is suggested to isolate the parked in the garage cars in pairs by which will be operating a thick curtain of water at arisen burning. The necessary insulation for solid noncombustible barriers are replaced at this way [3–6].

2.1 Operating principal

Referring to **Figure 1**, cars are placed to ensure the possibility between the pairs to have enough distance for the implementation of water curtains. In case of burning over the car is formed upward convective flow, because of differences of the density of the products of combustion and the environment. This stream is proportional to the lift force:

$$dF_A = -\left[\int_f (\rho - \rho_{ok}) g df\right] dx, \tag{1}$$

where f is the area of fire ignition and dx is elementary stretch in the vertical direction.

The power of convective updraft is determined by the number of Archimedes:

$$Ar = \left(\frac{\rho_{ok}}{\rho} - 1\right)\frac{g d_h}{u_0^2}, \tag{2}$$

where d_h is the hydraulic diameter of the outbreak of fire and u_0 is the initial value of the velocity of the upward flow. The velocity is determined according to [6]:

$$u_0^2 = 1,9 Q^{1/5}, \tag{3}$$

where Q, kW is the power of the fire.

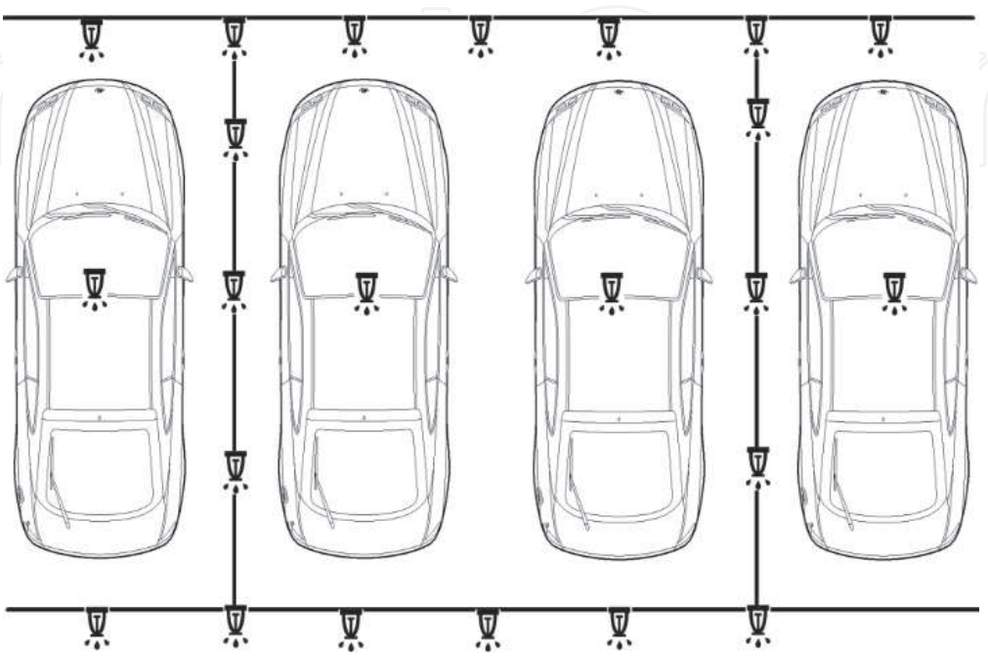

Figure 1.
Distribution of cars in the garages.

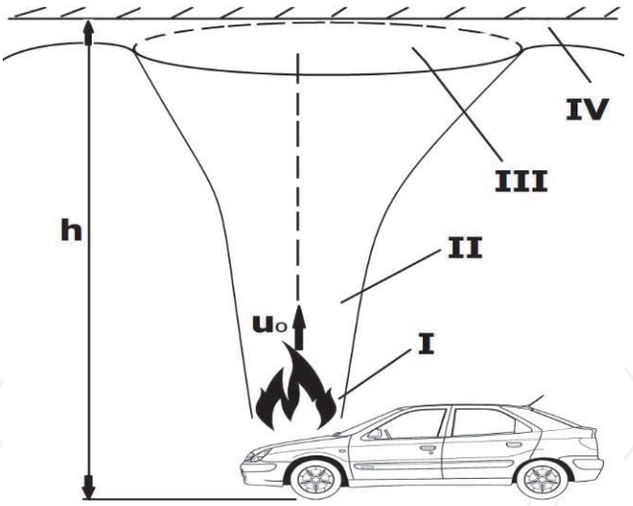

Figure 2.
Distribution of the fire.

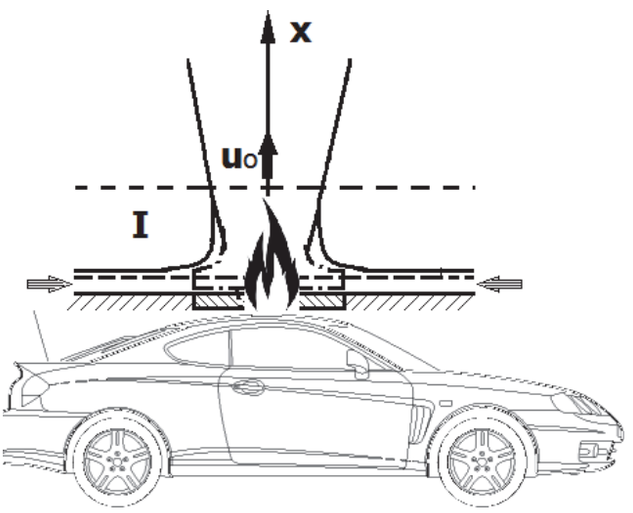

Figure 3.
Sketch of the convective flow.

The convective flow that is formed is shown in **Figure 2**. The conditional flow can be divided into the following areas: Convective flow is formed in zone I (**Figure 3**). The ambient air enters the fire zone from all directions, which heats and reverses the direction vertically. The second zone is a free convective flow that continues until it reaches the ceiling of the room where the flow changes character (zone III). In this zone, the jet is transformed into a radially semi-enclosed stream and spreads over the garage ceiling (zone IV).

The system includes fire sprinklers—quick response and standard sprinklers. Convective flow is reaching the garage ceiling under the influence of its temperature and a quick response sprinkler is switched on and the burning car is flushed with a water spray. Thus begins the process of extinguishing a fire in the initial stages. Further, propagating as a radial semi-closed jet, it reaches the "standard" reaction sprinklers that are included on the water curtain [7, 8].

This stage is defined as the isolation of burning cars from the surrounding area and no other pairs are affected.

2.2 Mathematical model of convective non-isothermal jet

For the purpose of solving the task is used an integral method according to [9, 10]. The used equations are as follows [11–13]:

- for amount of movement

$$\frac{d}{dx}\int_0^b \rho u^2(\pi y^j)dy = -g\int_0^b (\rho - \rho_{ок})(\pi y)^j dy \tag{4}$$

- to preserve enthalpy flow

$$\frac{d}{dx}\int_0^b \rho \Delta h u y^j dy = 0 \tag{5}$$

- for export of vertical upward mass flow

$$\frac{d}{dx}\int_0^b u(\rho - \rho_{ок})(\pi y)^j dy = 0 \tag{6}$$

A simple solution can be made as (5) of enthalpy is replaced by a linear dependence on the widening of the jet

$$b = cx \tag{7}$$

On the right-hand side of Eq. (4) is written the Archimedes buoyancy. The significance of included symbols is as follows: u is the jet velocity; y is the transverse coordinate; ρ is the current density; $\rho_{ок}$ is the density of the environment; and Δh is the enthalpy of the stream. The exponent j signifies: at j = 0 a flat stream and j = 1 an axis jet. The coordinate x is directed vertically upward.

There is a correlation between density and temperature:

$$\rho = \frac{p}{RT}, \tag{8}$$

where p is the pressure of the environment, R is the gas constant, and T is the absolute temperature. Similarity to transverse distribution of the velocity and the density (temperature) are initiated [1, 2], where solving Eqs. (4) and (6) leads to the parameters of the upward convective stream:

- the velocity of the upward stream

$$u_m = B''_u D_0^{1/3} \Delta T_{пл}^{4/9} \overline{x}^{1/3} \tag{9}$$

- the temperature difference

$$\Delta T_m = T_m - T_{env} = B''_{\Delta T} D_0^{1/3} \Delta T^{8/9} \overline{x}^{5/3}, \tag{10}$$

where D_0 is the initial diameter of the heat source of fire (the burning car); $\Delta T_1 = T_{fl} - T_{env}$; $\overline{x} = \frac{x}{D_0}$; the constants B''_u and $B''_{\Delta T}$ have values $B''_u = 0.222\left[m^3 K^{9/4}\right]$, $B''_{\Delta T} = 0.71\left[m^{1/3} K^{9/8}\right]$.

These values correspond to the case at $\overline{x} = \frac{x}{D_0} \geq 3 \div 3.5$. When adopted fire size created from a burning car $D_0 = 0.5$ m and height $H = 3 \div 4.5m$, $\overline{x}$ of the garage will be always greater than the above values.

At the relatively short distance to the ceiling, the high power of fire (the accepted conditions are $Q = 1500$W and $T = 600$K), the velocity and the temperature of the rising convective stream do not change significantly.

The initial velocity calculated by Eq. (3) is $u_0 = 8.2$ m/s and the time when the convective stream will reach the ceiling at different heights of the garage is given in **Table 1**.

This means that less than 1 s sprinklers over the burning car will be activated and extinguishing stream will flow over the burning car.

The expansion (increasing of thickness) of the jet in height can be determined by the expression:

$$\frac{db}{dx} = 0.22\frac{\rho_0 + \rho_{ок}}{2\rho_{ок}}, \tag{11}$$

where,

$$b = \left[0.22\frac{\rho_0 + \rho_{ок}}{2\rho_{ок}}\right] \tag{12}$$

The density of the jet in the opening section is defined by Eq. (8): at $R = 287$ J/kgK, $T_0 = 600$ K, $p = 10^5$Pa in which for ρ_0 is received $\rho = 0.58$ kg/m^3. The density of the environment is $\rho_{env} = 11.2$ kg/m^3 at the same pressure and temperature $T_{env} = 293$ K. At this density, the widening of the jet in the present case is

$$b = 0.163x \tag{13}$$

For a different height in the garage, the parameter b is given in **Table 2**.

The last row in **Table 2** is given the extension of the isothermal jet($T_0 \approx T_{env}$). Obviously a slight extension of non-isothermal convective flow comparing with the isothermal.

Reaching the ceiling vertical, the convective stream is transformed into radial jet (**Figure 4**).

h, m	3	3.5	4	4.5
Δt	0.36	0.43	0.49	0.55

Table 1.
h—height of the garage, m; Δt—time of the fire to reach the ceiling, m.

h (m)	3	3.5	4	4.5
b_1 (m)	0.501	0.507	0.652	0.73
b_{sou} (m)	0.651	0.77	7.74	1.98

Table 2.
h—height of the garage, m; b_o—initial width of the radial jet, m; b_1—width of the radial jet, m.

Due to the weak widening of the jet and the short distance to the ceiling, the mass flow is not increased significantly because the temperature, density, and relatively low mileage ceiling have not changed. The jet has retained its temperature and density, and the velocity according to [14] may be determined:

$$u_{\max} = 0.88u_0, \tag{14}$$

where for $u_0 = 8.2$ m/s it is $u_{\max} = 7.2$ m/s.

It is assumed that the starting size of the radial jet is equal to that obtained in **Table 2**, b_1, that is $D_0 = b_1$.

Width of the radial jet b_0 is determined by the flow rate Q at the intersection of the reverse flow. The flow rate is amount of initial flow rates Q_0 and increase its height due to suction of air from the environment. The flow rate of ejecting fluid is considered proportional to the square of the relative increase in the width of the jet $\left(\frac{b_1-b_0}{b_0}\right)^2$ and the distance x divided by the duration of the process Δt.

$$Q_{ej} \approx \left(\frac{b_1 - b_0}{b_0}\right)^2 \frac{x}{\Delta t}, \mathrm{m}^3/\mathrm{s} \tag{15}$$

In this, total flow rate is obtained as the sum of normal and ejecting flow rate:

$$Q = Q_0 + Q_{ej}, \mathrm{m}^3/\mathrm{s}, \tag{16}$$

where $Q_0 = u_0 \frac{\pi d_n^2}{4}$, when $d_n = 0.5$ m and $u_0 = 8$ m/s we have:

$$Q = Q_0 + Q_{ej} = u_0 \frac{\pi d_n^2}{4} + \left(\frac{b_1 - b_0}{b_0}\right)^2 \frac{x}{\Delta t} \tag{17}$$

The flow rate of the respective heights $x = 3; 3.5; 4; 4.5$ m of the garage is shown in **Figure 5** where it is defined by the relationship given in Eq. (12), respectively and in case of a leak by Eq. (13).

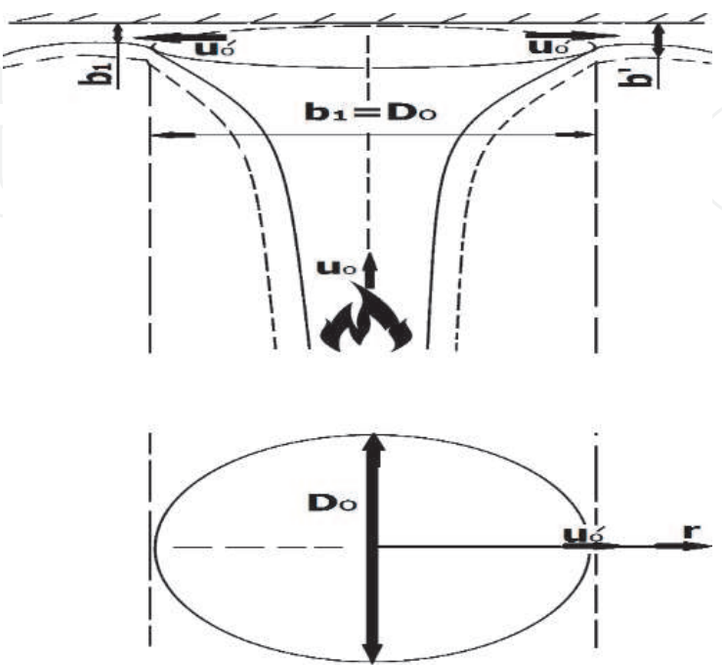

Figure 4.
Sketch of radial jet.

According to **Figure 4**, it is assumed $D_0 = b_1$ that is already known and for flow rate in Eq. (16), the original width of the radial jet b'_0 is calculated:

$$b'_0 = \frac{Q}{\pi D_0}. \tag{18}$$

The relationship $b_0(x) = f(x)$ is given in **Figure 6**.

The cross-section of the radial jet as a function of r is determined by the expression:

$$S = 2\pi r b', \tag{19}$$

where r is the current radius, b' is the width of the jet to the corresponding r.

Since the resulting stream is parietal and has parietal boundary layer whose thickness is approximately $0.1b'$, Eq. (19) can be recast in the form:

$$S = 2.2rb' \tag{20}$$

The width b' is calculated by Eq. (12) and for the case in Eq. (13) by replacing x with r, then we have:

$$b' = \left[0.22\frac{\rho_0 + \rho_{ok}}{2\rho_{ok}}\right]r = c'r; c' = 0.22\frac{\rho_o + \rho_{ok}}{2\rho_{ok}}, \tag{21}$$

respectively, $b' = 0.163r$.

When substituted in Eq. (19) we get the following:

$$S = 2.2\pi c' r^2 \tag{22}$$

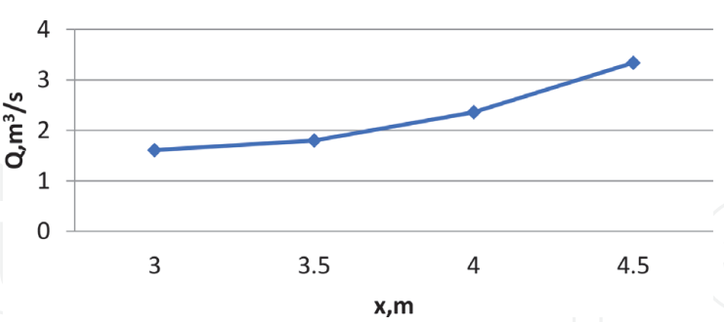

Figure 5.
Change of the flow rate at different heights of the garage.

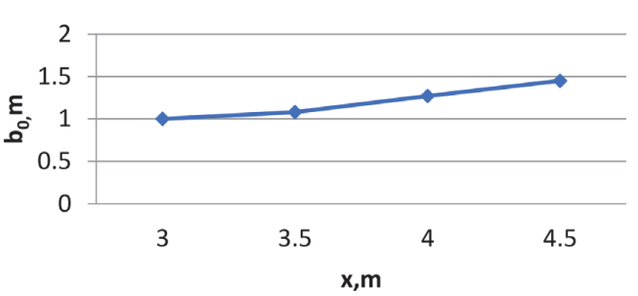

Figure 6.
Change of the initial weight at different heights of the garage.

The average velocity of the ceiling of the room depending on r is obtained by:

$$u_m = \frac{Q}{S}, \tag{23}$$

respectively:

$$u_m = \frac{Q}{2.2\pi c' r^2}, \text{m/s} \tag{24}$$

Parking average velocity depending on r at the four heights is shown in **Figure 7**. **Figure 8** shows the time to reach the appropriate distance:

$$\Delta t = \frac{r}{u_m}, \text{s} \tag{25}$$

This means that in the first 2 s, all sprinklers at distance of 2 m away from the burning car will be triggered. For longer distances, the remote sprinklers will act at a condition if the temperature of the burning car does not decrease too quickly. For maximum calculated time of 7.7 s could not be expected too much decrease of the temperature, which leads to the conclusion that the ceiling temperature will be much greater than the starting temperature of "fast" sprinklers so that at $t_p = 57°C$ or T = 330°K will always remain less than the temperature of the wall jet which initial temperature is 600°K.

With the removal from the water curtain, it is possible to turn on the other ceiling sprinklers that are in the range.

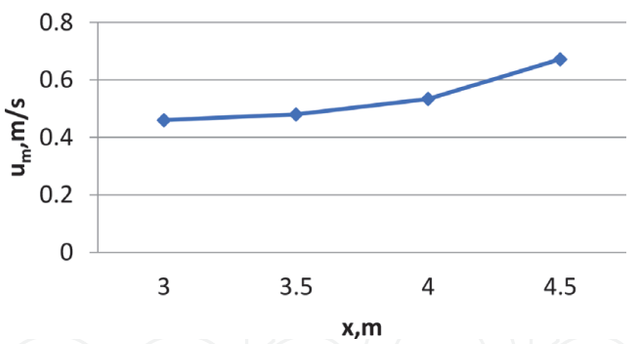

Figure 7.
Average velocity at different heights of garage.

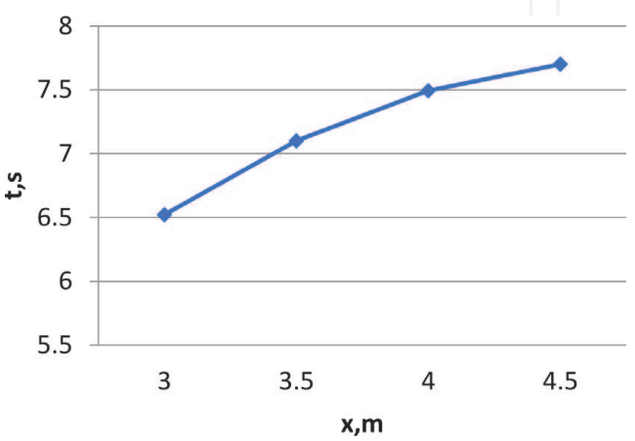

Figure 8.
Time to reach the sprinklers at different heights of garage.

In the vicinity of the burning car to sprinkler curtain, a distance of $l \leq 2$ m will trigger three (to five) fast sprinklers. At a longer distance, it will trigger maximum of three quick sprinklers of water curtain plus the main ones over the burning car and eventually those are lying in the range of $l = 4$ m ceiling sprinklers so that the number of activated sprinklers will increase [10].

To create a smokeless zone under a layer of smoke floating [14], air exhaust systems are designed and installed for smoke and hot gases. An exhaust ventilation system for smoke and hot gases is a scheme of safety equipment designed to perform a positive role in spin fire. The smoke is drawn in the direction of the noncarrier partition EI from a velocity of 2 m/s to 5 m/s. Standard allowed velocity of 5 m/s, but it should be taken into consideration that this velocity would affect negatively and lead to the merging of streams of pure air.

From Abramovich [14], the density of the thermal load in the premises for the storage of combustible materials according to their purpose, is determined the heat capacity of the prevailing materials. The ventilation system to remove smoke and heat (VSRSH) has to reach its designed performance level within 60 s of receiving the command signal. Each VSRSH has to ensure receipt of sufficient fresh air that enters the room for the expense of the flue products.

2.3 Thermal impact

Heat transfer by convection and radiation is defined according to [3, 10]. Thermal effects are expressed by the intensity of the heat flow h_{nbt}, $\mathrm{W/m^2}$ to the surface of the element is determined taking into account the heat transfer by convection and radiation, such as:

$$h_{nbt} = h_{nbt,c} + h_{nbt,r}, \mathrm{W/m^2}, \tag{26}$$

where heat transfer by convection $h_{nbt,c}$ is given by the relationship

$$h_{nbt,c} = \alpha_c\left(\theta_g - \theta_m\right), \mathrm{W/m^2} \tag{27}$$

radiation heat transfer $h_{nbt,r}$ is given by the dependence:

$$h_{nbt,r} = \Phi\varepsilon_m\varepsilon_f\sigma\left[(\theta_1 r + 273)^2 - (\theta_m + 273)^4\right], \mathrm{W/m^2} \tag{28}$$

Convection component of the intensity of the heat flow is determined by:

$$h_{nbt,t} = \alpha_c\left(\theta_g - \theta_m\right), \mathrm{W/m^2} \tag{29}$$

where α_c is the heat transfer coefficient by convection $\left[\frac{\mathrm{W}}{\mathrm{m^2}}\mathrm{K}\right]$; θ_g is the gas temperature near the exposed fire element [°C]; and θ_m is the surface temperature of the element [°C].

The coefficient of heat transfer by convection α_c is determined by the nominal curves corresponding to "temperature–time." On indirectly heated surface elements, the intensity of heat flow h_{nbt} is determined by Eq. (16) where $\alpha_c = 4\left[\frac{\mathrm{W}}{\mathrm{m^2}}\mathrm{K}\right]$. The coefficient of heat transfer by convection has value $\alpha_c = 9\left[\frac{\mathrm{W}}{\mathrm{m^2}}\mathrm{K}\right]$, considering that the effects of heat transfer by radiation are included.

Radiating components of net heat flux per unit surface area are defined as $h_{nbt,r} = \Phi\varepsilon_m\varepsilon_f\sigma\left[(\theta_1 r + 273)^2 - (\theta_m + 273)^4\right], \mathrm{W/m^2}$, where: Φ is the factor of configuration,

ε_m is the emitting surface element, ε_f the transmission of fire, $\sigma = 5.67 \times 10^8 \left[\frac{\text{WK}^4}{\text{m}^2}\right]$ is the constant of Stefan-Boltzmann, θ_r is the effective temperature of the radiation environment [°C], and θ_m is the surface temperature of the element [°C]. Transmission of fire is equal to $\varepsilon_f = 1$.

2.4 Determination of the intensity of water curtain

Because of the difficulties associated with the construction of fire walls, experiments are conducted so that these areas to be reduced to such proportions that the primarily split up do not disturb of the process. In many cases, such as in buildings of first degree of fire resistance, as already noted, firewalls did not provide the detriment of fire safety. In connection with this arises a need of using such fire barriers that could effectively limit the spread of fire and at the same time would give some freedom for internal layout of buildings with different functions, which is the case of the water curtain [15].

When calculating water curtains, the assumption must simultaneously satisfy the following conditions:

Structural parts of the building to withstand the effects of fire on one side and the passage of flames or hot gases to be prevented by the transfer of heat to the unexposed side. The ability of the structural parts of the building to withstand the effects of fire on one side and prevent the transfer of heat from the exposed to the unexposed side. The transfer is limited so that it does not ignite either the unexposed surface, or any other material in the immediate vicinity. The structural element is designed to serve as a barrier against the heat and to ensure the protection of people who are close to it.

The effectiveness of water curtains is assessed according to the amount of absorbed heat.

It is known that the dependence of the growth temperature of the source of radiation of maximum energy moves to the side of the shorter waves. This follows from the law of Vin:

$$\lambda_{\max,T} T = 0.29 = const \tag{30}$$

where λ is the wavelength in m, T is the temperature at the surface of water curtain, °K.

Good enough inter-phase and heat-absorbing surfaces have water drops of size 200×10^{-6}. It is considered that in the best case, sprinklers spray water of size less then 1000 μm.

2.5 Required flow rate for air curtain

The current has the following characteristics: density of the radiation heat flux is 1500 W/m^2; density of the irradiation protected material is 900 W/m^2; height of the hole–4 m; length of the hole–6 m; pressure of water in sprinkler–0.6 MPa (6 atm) and the radius of the water drops–0.0006 m (600 μm).

Opacity density of the curtain:

$$\delta = \frac{2.303 \log q_{изл}}{q_{кр}} = 0.51 \tag{31}$$

Thickness of the curtain:

$$R = \frac{\delta}{c} = \frac{0.51}{2.8} = 0.182 \text{ m} \tag{32}$$

Flow rate of the water curtain for 1 m^2 of lateral surface is defined by:

$$Q = 0.666\mu\rho\frac{rR}{H}\sqrt{2gh} = 0.467\frac{l}{s} \text{ m}^2 \tag{33}$$

For the whole surface of the water curtain:

$$Q^H = 11.2l/s \tag{34}$$

Water curtains are constructed so that the entire hole is irrigated with finely dispersed water. For this purpose, sprinklers are placed over the hole and next to it. When they are placed at the top of the hole, it is possible for unprotected areas to remain through which it is possible for a penetration of hot gases to occur.

Sprinkler heads that are used to spray jets are spaced 0.5 m in protecting small holes and 1.25–1.5 m in protecting large holes. For sprinkler heads which are situated at a distance greater than 3 m, it is required head pressure of the water 4–6 mH_2O.

3. Numerical simulations: mathematical model of flow in a confined space

The mathematical model is based on the equations used in the computational mechanics of fluids. These are the continuity equations, the Navier-Stokes equations in modification according to the Businex hypothesis ($\mu_{eff} = \mu + \mu_t$), the energy equation (1st law of Thermodynamics), the Clapeyron equation for the gas mixture. Fire currents run at low speeds in the absence of detonation and explosions.

In the case of a fire without detonation, combustion, and explosions, it can be assumed: $div\vec{V} = 0$, $\frac{\partial u}{\partial x} + \frac{\partial v}{\partial y} + \frac{\partial w}{\partial z} \equiv 0$.

To these are added the equations for smoke propagation (smoke content) and for the optical density of the gas mixture.

Continuity equation:

$$\frac{\partial \rho}{\partial t} + \frac{\partial(\rho u)}{\partial x} + \frac{\partial(\rho v)}{\partial y} + \frac{\partial(\rho w)}{\partial z} = J \tag{35}$$

Equations for movements [9].

$$\rho\frac{\partial u}{\partial t} + \rho u\frac{\partial u}{\partial x} + \rho v\frac{\partial u}{\partial y} + \rho w\frac{\partial u}{\partial z} = -\frac{\partial p}{\partial x} + \mu\left(\frac{\partial^2 u}{\partial x^2} + \frac{\partial^2 u}{\partial y^2} + \frac{\partial^2 u}{\partial z^2}\right) + 2\frac{\partial}{\partial x}\left[\mu_T\frac{\partial u}{\partial x}\right] + \frac{\partial}{\partial y}\left[\mu_T\left(\frac{\partial u}{\partial y} + \frac{\partial v}{\partial x}\right)\right] + \frac{\partial}{\partial z}\left[\mu_T\left(\frac{\partial u}{\partial z} + \frac{\partial w}{\partial x}\right)\right] \tag{36}$$

$$\rho\frac{\partial v}{\partial t} + \rho u\frac{\partial v}{\partial x} + \rho v\frac{\partial v}{\partial y} + \rho w\frac{\partial v}{\partial z} = -\frac{\partial p}{\partial y} + \mu\left(\frac{\partial^2 v}{\partial x^2} + \frac{\partial^2 v}{\partial y^2} + \frac{\partial^2 v}{\partial z^2}\right) + 2\frac{\partial}{\partial y}\left[\mu_T\frac{\partial v}{\partial y}\right] + \frac{\partial}{\partial x}\left[\mu_T\left(\frac{\partial u}{\partial y} + \frac{\partial v}{\partial x}\right)\right] + \frac{\partial}{\partial z}\left[\mu_T\left(\frac{\partial v}{\partial z} + \frac{\partial w}{\partial x}\right)\right] \tag{37}$$

$$\rho\frac{\partial w}{\partial t}+\rho u\frac{\partial w}{\partial x}+\rho v\frac{\partial w}{\partial y}+\rho w\frac{\partial w}{\partial z}=-\frac{\partial p}{\partial z}+\mu\left(\frac{\partial^2 w}{\partial x^2}+\frac{\partial^2 w}{\partial y^2}+\frac{\partial^2 w}{\partial z^2}\right)+2\frac{\partial}{\partial z}\left[\mu_T\frac{\partial w}{\partial z}\right]+\frac{\partial}{\partial x}\left[\mu_T\left(\frac{\partial u}{\partial z}+\frac{\partial w}{\partial x}\right)\right]+\frac{\partial}{\partial y}\left[\mu_T\left(\frac{\partial v}{\partial z}+\frac{\partial w}{\partial y}\right)\right] \tag{38}$$

Equations for heat exchange (1st law of Thermodynamics)

$$\rho C_p\left(\frac{\partial T}{\partial t}+u\frac{\partial T}{\partial x}+v\frac{\partial T}{\partial y}+w\frac{\partial T}{\partial z}\right)=\frac{\partial}{\partial x}\left[\left(\lambda+\lambda_t+\lambda_f\right)+\frac{\partial T}{\partial x}\right]+\frac{\partial}{\partial y}\left[\left(\lambda+\lambda_t+\lambda_f\right)+\frac{\partial T}{\partial y}\right]+\frac{\partial}{\partial z}\left[\left(\lambda+\lambda_t+\lambda_f\right)+\frac{\partial T}{\partial z}\right]+q+\varepsilon \tag{39}$$

where c_p is the specific heat content at constant pressure; λ is the coefficient of thermal conductivity; λ_i is the coefficient of turbulent thermal conductivity; λ_p is the coefficient of radiation thermal conductivity; and q_v is the intensity of internal heat sources.

Here, q_v, can be represented by $q_v = q_{vc} + q_{vr} + q_{vb}$, where q_{vk} is the intensity of internal convective heat sources; q_{vb} is the intensity of internal combustion sources; and q_{vr} is the intensity of internal sources due to radiation heat transfer.

Gas condition equation is given by:

$$p = \rho TR, \tag{40}$$

where R is the universal gas constant.

Law for the conservation of the mass of the ith gas that is a part of the mixture is

$$\rho\frac{\partial \chi_i}{\partial t}+\rho u\frac{\partial \chi_i}{\partial x}+\rho v\frac{\partial \chi_i}{\partial y}+\rho w\frac{\partial \chi_i}{\partial z}=\frac{\partial}{\partial x}\left(\rho D\frac{\partial \chi_i}{\partial x}\right)+\frac{\partial}{\partial y}\left(\rho D\frac{\partial \chi_i}{\partial y}\right)+\frac{\partial}{\partial z}\left(\rho D\frac{\partial \chi_i}{\partial z}\right)+m_i, \tag{41}$$

where D is the diffusion coefficient, representing the sum of the coefficient of gas diffusion D_i and the coefficient of turbulent diffusion $D_t (D = D_i + D_t)$; χ is the mass concentration of the ith gas; m_i is the intensity of internal mass sources arising from the formation (disappearance) of molecules of a gas, a consequence of the ongoing chemical reactions of combustion in fires.

The law (equation) for preserving the optical density of smoke is of the form:

$$\frac{\partial D_{on}}{\partial t}+u\frac{\partial D_{on}}{\partial x}+v\frac{\partial D_{on}}{\partial y}+w\frac{\partial D_{on}}{\partial z}=q_D, \tag{42}$$

where D_{on} is the smoke-generating capacity of the combustible material and q_D is the intensity of the internal sources of optical density of the smoke formed by the ongoing reaction of combustion in a fire [3].

The thermophysical parameters of the mixture of gases involved and the result of combustion in a fire take into account the chemical composition of this mixture. It consists of oxygen, nitrogen, and combustion products - carbon monoxide, nitrogen, sulfur, etc., involved in the process combustible ingredients. They are defined as follows:

- density of the mixture

$$\rho = \sum_{i-1}^{n} \alpha_i \rho_i \tag{43}$$

- gas constant

$$R = \sum_{i-1}^{n} \chi_i R_i \tag{44}$$

- specific heat capacity

$$c_p = \sum_{i-1}^{n} \chi c_{p_i}, \tag{45}$$

where α_i is the bulk concentration of the ith component and $\mathcal{H}_i$ is its mass concentration.

The values of these parameters are determined at constant pressure ($p = const$). They can be considered as temperature dependent or considered permanent.

3.1 A characteristic equation

The characteristic equation summarizes the main partial differential equations, which are solved sequentially in software for each of the flow parameters. The type of equation is as follows:

$$\frac{\partial}{\partial x}(\rho\Phi) + div(\rho w\Phi) = div(\Gamma grad\ \Phi) + S, \tag{46}$$

where Φ is the dependent variable—velocity components, enthalpy, concentration of the components of the gas medium, optical density of the smoke, respectively; Γ is the diffusion coefficient for the corresponding Φ; and S is the source member. The values for Eq. (46) are given in [9].

3.2 Modeling the turbulence using CFD

Most often, a CFD-Fluent turbulence $k - \varepsilon$ model is applied. In this model, the coefficient of turbulent viscosity υ_t is represented by the Kolmogorov-Prandtl dependence, as the ratio of kinematic turbulent energy k and the rate of dissipation ε:

$$\upsilon_t = C_\mu \frac{k^2}{\varepsilon}, \tag{47}$$

where

$$k = \frac{1}{2}\sqrt{u'^2 + v'^2 + w'^2}; \qquad \varepsilon = \upsilon \overline{\left[\left(\frac{\partial u}{\partial x}\right)^2 + \left(\frac{\partial v}{\partial y}\right)^2 + \left(\frac{\partial w}{\partial z}\right)^2\right]} \tag{48}$$

3.3 FDS turbulence modeling

To close the system of equations at FDS, as in all other cases in turbulent flows, it is necessary to use appropriate models of turbulence. In this case, the large eddy

simulation model [9] known in this type of task as the LES model is recommended as the most appropriate. The model is described in detail in [9].

The model of large eddy simulation is based on the following: large-scale vortices differ markedly in the course of transition from one current to another, with the small-scale structure changing slightly. The field of large-scale structures needs to be defined. Continuity of flow parameters is assumed using Leonard's so-called filtering function. For each flow parameter, $a = a + a'$. Dissipative combustion processes such as viscous thermal conductivity, diffusion, and impurity transfer are modeled. What is special about the model is that the scale of the vortex structures is smaller than the size of the data network. The parameters μ, λ, and D in the equations describing the process are replaced by expressions modeling their effect.

The strain rate tensor is used to determine μ. Thermal conductivity and impurity diffusion are determined by:

$$\begin{aligned} \lambda_t &= \frac{\mu_t c_p}{pr_t} \\ (\rho D)_t &= \frac{\mu_t}{S_{0t}} \\ \mu_t &= \rho v_t \end{aligned} \tag{49}$$

In the case of laminar heat transfer and diffusion, respectively:

$$\begin{aligned} \lambda &= \frac{\mu c_p}{pr} \\ (\rho D) &= \frac{\mu}{S_{0t}} \end{aligned} \tag{50}$$

The process of combustion in the fire is most often implemented using the "Part of the mixture" approach. It is a scalar quantity characterizing the mass concentration of one or more components of a gas mixture at a given point in the flow. To reduce the volume of calculations, the significant memorized are two components of the mixture: mass concentration of unburned fuel and burned, respectively. Combustion products. Radiant heat transfer is calculated by the equations for the emission of sulfur-containing gases, which, in fact, implies a constraint on the problem. Large-scale models may also be used in certain cases. FDS equations use the FVM finite volume method. In addition to using the LES turbulence model, successful attempts have been made to apply the direct numerical modeling method described in [9]. FDS has been tested in a number of laboratories and institutions in the United States. The validation done shows the possibility of its application in many cases [16].

4. Computer modeling and numerical simulations

A detailed description of the Fluent (CFD) program interface is given in [17–19].

Development of fire in atrium space: The development of fire occurred in a certain object—the building shown in **Figure 9** and **Figure 10**, located on Tsarigradsko shose Blvd., Sofia.

The arrangement of the air exchange in the atrium space in case of fire is shown in **Figure 10**. Atrium air exchange was implemented, showing zones with critical parameters of radiation, smoke, and fire. It is important to note that all of the above is possible only by knowing the respective velocity or temperature field of the air in the room [5].

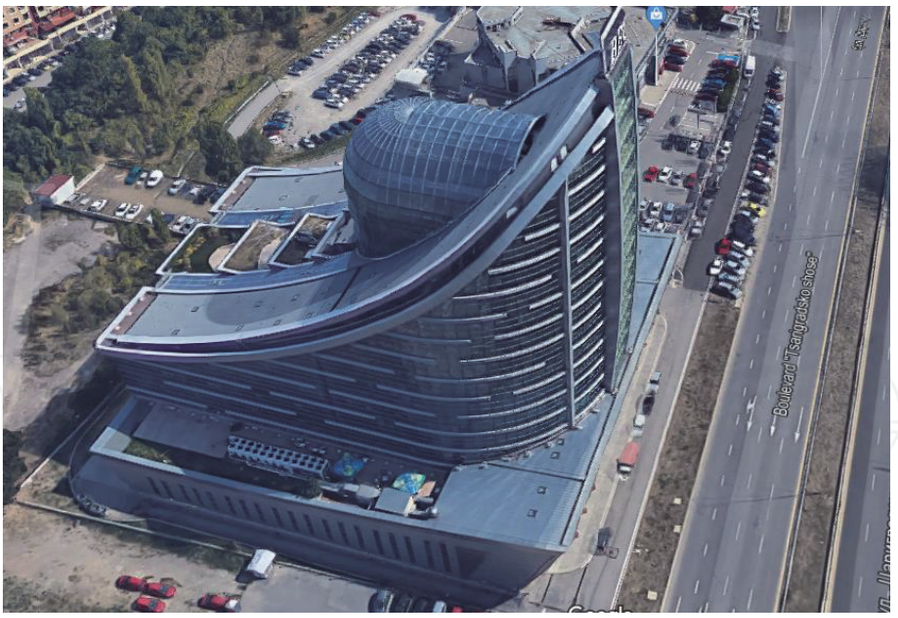

Figure 9.
Building with atrium subject to simulation study [20].

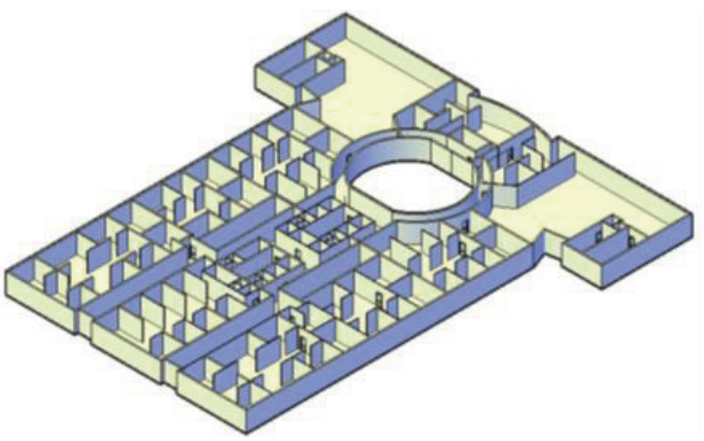

Figure 10.
Building fire development.

The geometric model so drawn shows the location of the fire, that is, hazard generator and flue gas outlet (smoke hatches).

In real fires, there is a degree transition zone between lower cold smoke and higher hot smoke.

The first smoke curtain signal may be calculated from the beginning of the transition zone formation. Thus, it can be assumed that forecasts using equations of this type depend on the exact application of the computer model.

After the 3D Atrium Model has been built (in the Gambit work environment), it is necessary to proceed with the "networking" procedure of the volume. Due to the large volume, it is not appropriate to use crosslinking of the elements in the same step.

For this reason, a fine mesh is selected at the site of fire generation and its departure from the room, while a larger one is used far from them.

In the present case, triangular elements were selected for the site of fire generation and the smoke hatches for the networking of persons with step 0.3 m. For the other walls as well as the volume of the atrium, a step of 0.5 m is chosen.

Figure 11 shows the velocity field in the atrium in vector form. It can be seen from the figure that high velocities are observed at the site of smoke generation, both near the walls and the high part of the atrium.

The temperature distribution in the volume of the atrium is shown in **Figure 12**. Areas with higher temperatures are clearly visible—near the source of smoke and the surrounding wall above it, and near the dome of the atrium.

Figure 13 shows the distribution of smoke in the atrium at various points in time for 120 s until equilibrium between the ascending and descending currents in the atrium is reached.

Figure 14 shows the change in turbulent kinetic energy in the atrium. What is striking is the fact that there is an intense transfer of substances from the outbreak of the fire along the wall of the atrium to the dome, and then it slowly subsides. When smoke reaches the floor of the room, the turbulent kinetic energy is approximately zero.

Modern computer programs for numerical modeling of processes related to the simulation of air exchange in atriums can alleviate some regulatory requirements for protected premises (atriums), which can lead to significant savings for investors. If necessary, openings may be left open in the premises. With the use of fire ventilation, they will not have a negative effect on the parameters of the fire. In large areas, flue products may only be contained above the fire. The ability to make new, more practical, and economical architectural decisions is increasing.

Application of the FDS environment for predicting and restoring the spread of fires and damage in the building [21, 22].

An analysis is made in the FDS environment to look at the basic features on which it is based. In analyzing the program, it should be emphasized that it is related to the numerical mechanics of the fluids and software products built on this basis. The same system of private differential equations is used, with the difference between the CFD and the FDS medium in the equations used to describe the turbulence. Fluent programs utilize turbulence models, which narrows their applicability in the study of fires in unlimited space. Large Eddy Simulation (LES) is used for FDS. This expands the applicability in the study of currents and fires in open space, as well as the effect of wind, etc. Weather conditions when solving problems.

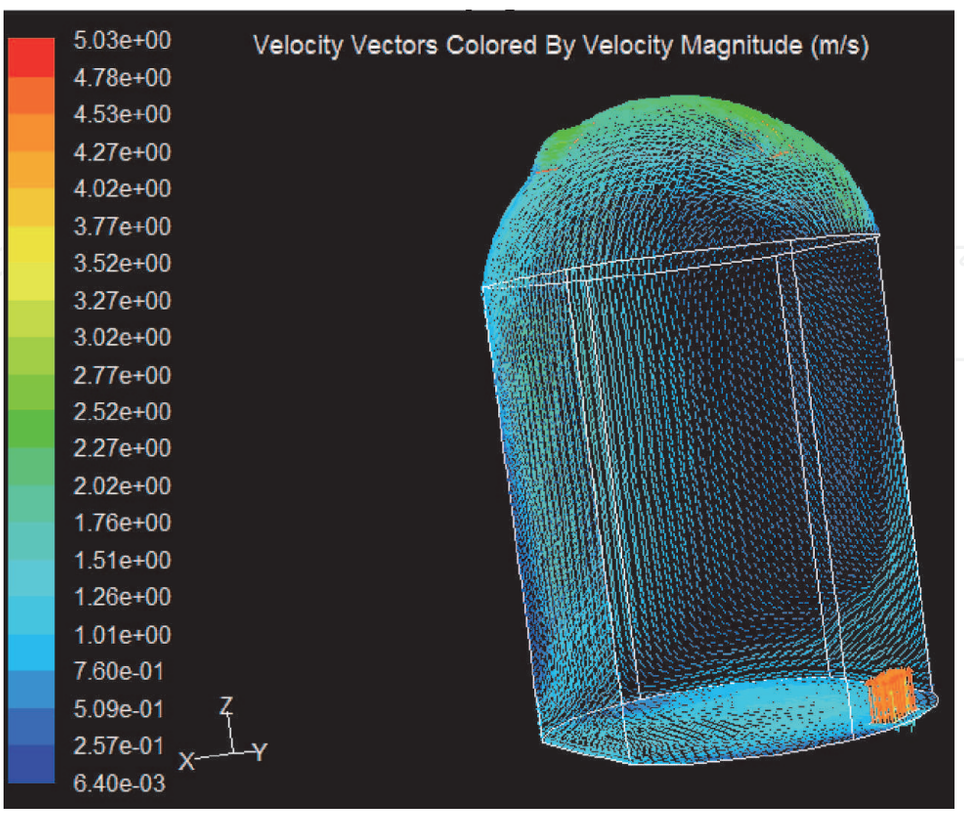

Figure 11.
The velocity field in atrium in vector form.

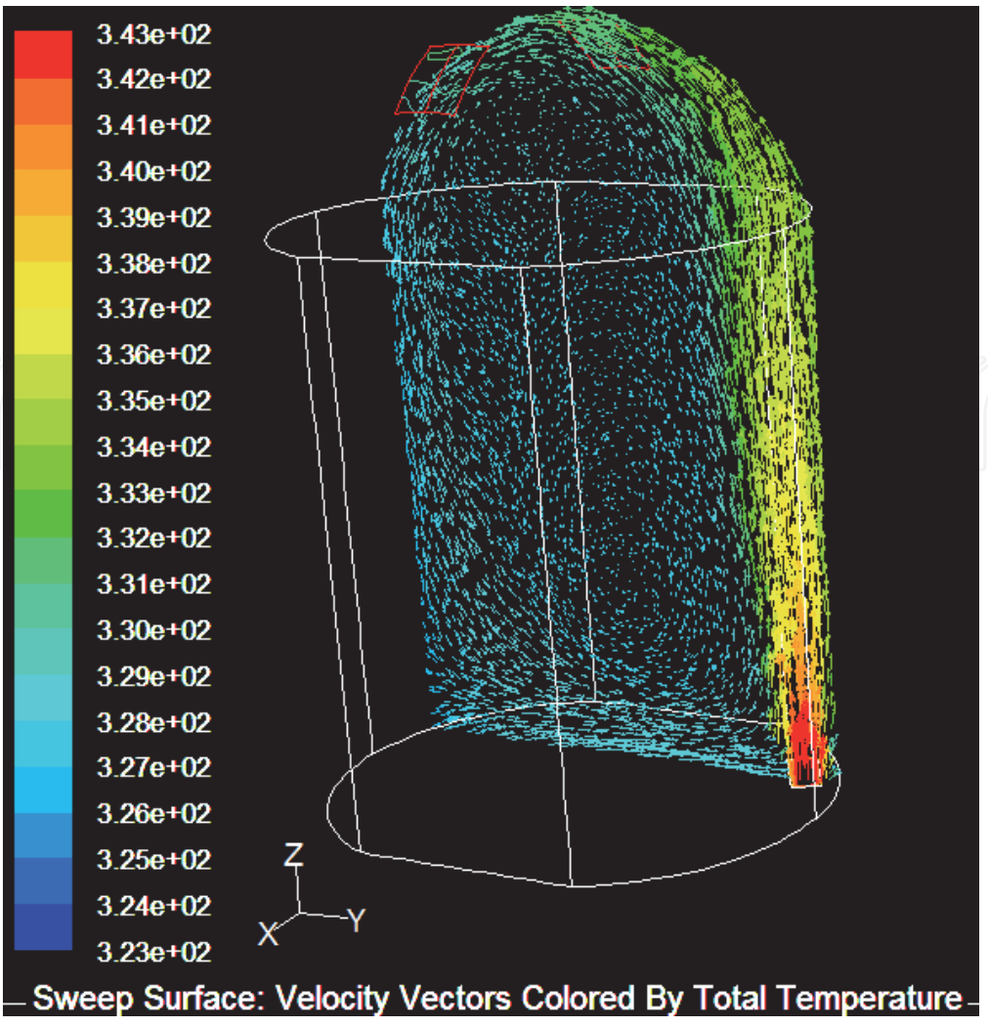

Figure 12.
The distribution of temperature in the volume of the atrium.

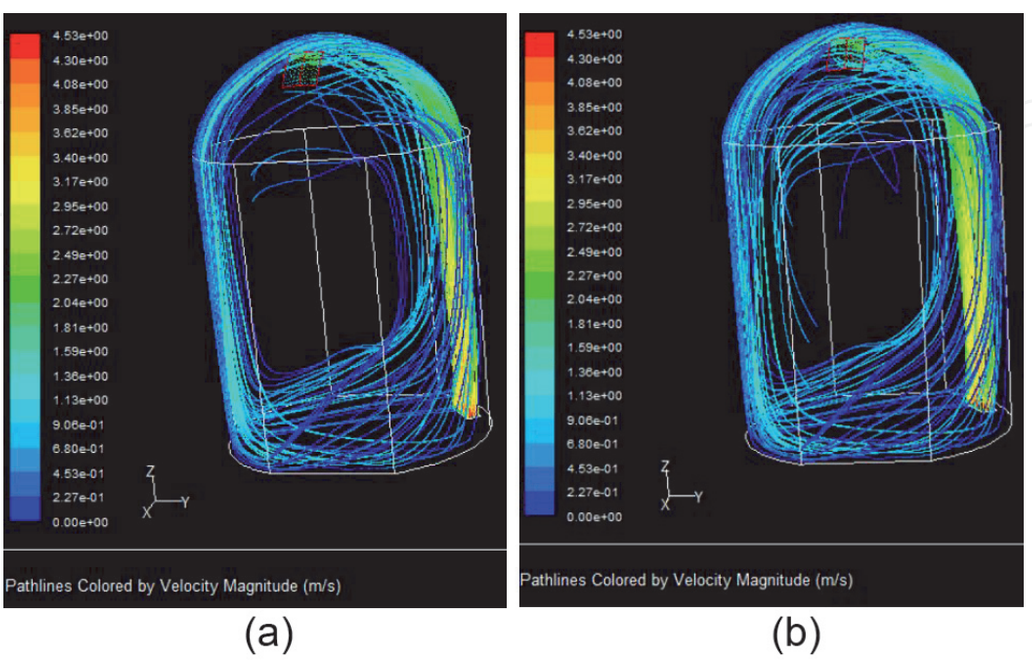

Figure 13.
The distribution of smoke in the atrium at different times. (a) 1320 s, and (b) 1440 s.

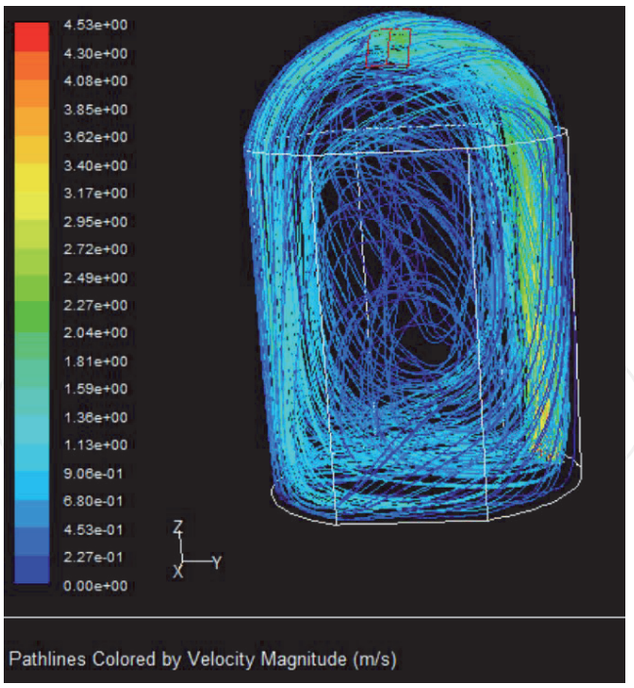

Figure 14.
Change in turbulent kinetic energy in the atrium.

The program is also used to analyze the spread of hazards in the work environment, both industrial and residential sites, as well as in the environment. This program allows to restore the development of fire in past events [5, 9, 16].

4.1 Closed-loop fire development modeling using the PyroSim (FDS) program

This simulation product is applicable to the modeling of fire development and the determination of the evacuation and extinguishing route indoors. The software environment offers intuitive function menus (graphical user interface) and provides results for the propagation of flue gases, hydrocarbons, and other substances during a fire, as well as the temperature distribution along the cross section of the model's geometry. The program serves not only the prediction of the situation, but also the investigation of fire in the setting of the initial ignition zone, as well as training. The simulations in the program are based on the computational dynamics of fluids, and in particular, low-velocity convective currents. The capabilities of the software make it possible to investigate fires from cooking stoves to oil derivative stores (oil bases). The program is also applicable to simulation of flame-free processes, including building ventilation testing.

A detailed description of how to work with the PyroSim interface is given in [17].

Development of fire in a training building: The development of a fire in study building 2 of TU-Sofia is investigated. The fire is assumed to start from the ground floor—one of the laboratories (**Figure 15**).

Specific examples of the application of the PyroSim software product are shown in **Figures 16–21** in a simulated fire in a training laboratory on the first floor of a technical building of the Technical University—Sofia. For the construction of the geometric model in **Figure 16**, the real barrier elements such as walls, doors, and windows, as well as the materials of which they are constructed with their respective melting/ignition temperatures, are taken into account.

Instantaneous flue gas images of the building are shown in **Figure 17** (for 50s), **Figure 18** (for 60s), and **Figure 19** (for 440 s). It is clear that the smoke is spreading

Figure 15.
Building 2 of TU-Sofia.

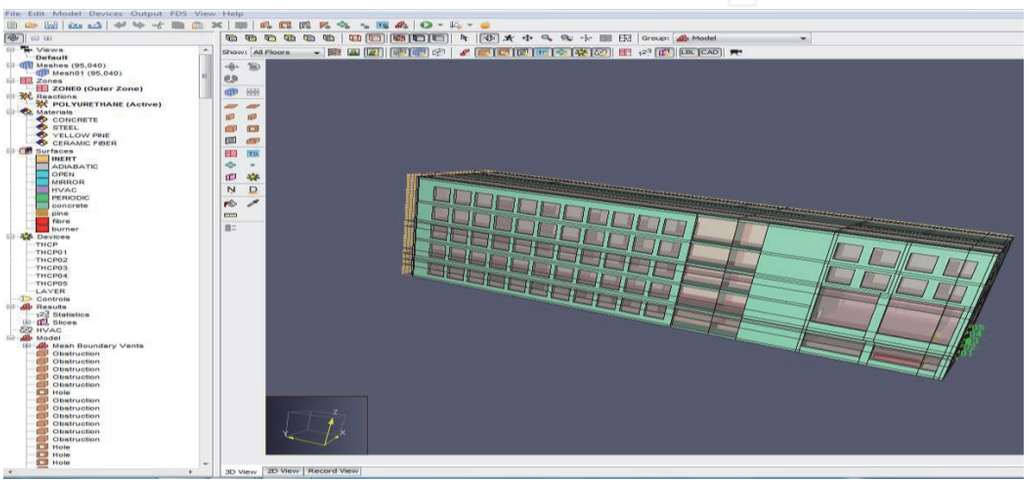

Figure 16.
Working environment for drawing the geometric model.

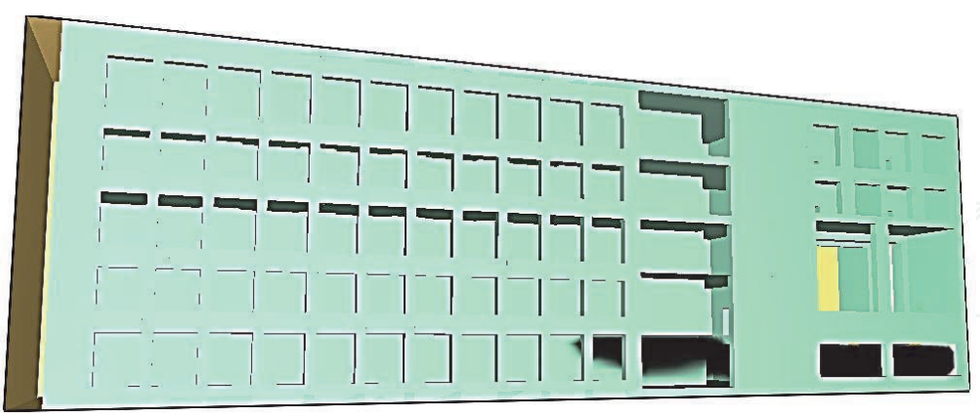

Figure 17.
Flue gas propagation in the building within 50 s of the simulation.

as fast as possible on one of the stairs, which is a kind of chimney (chimney) for this part of the building. For the same period of time, smoke spreads down the corridor on the first floor. Since there are no smoke barriers (doors) installed between the same staircase and the corridors on the floors, it will spread to all floors and will make it difficult to evacuate people in the building. Partition doors are placed on the next staircase (to the right of the model shown in **Figures 18** and **19**), which are intended to prevent the smoke from burning the floors in the direction from the staircase to the corridors, but in this case the flue gases will meet on both sides. The same barriers and

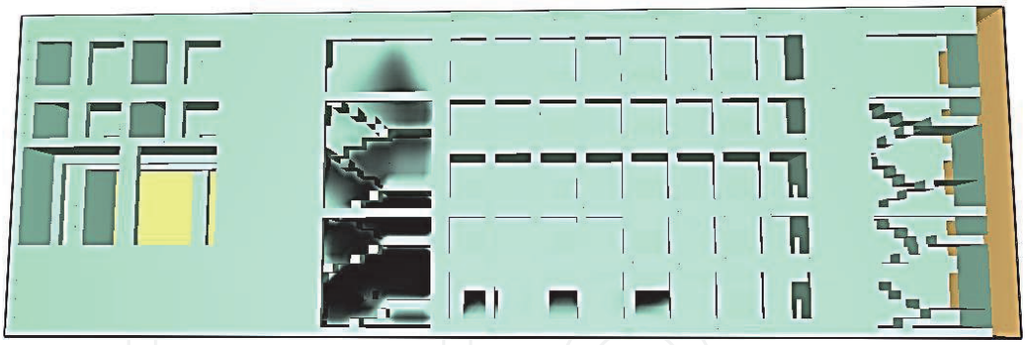

Figure 18.
Flue gas propagation in the building within 60 s of the simulation.

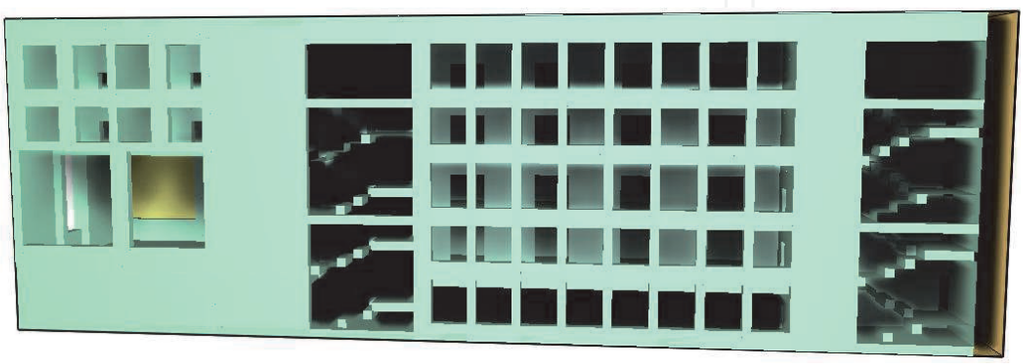

Figure 19.
Flue gas propagation in the building at 440 s of the simulation.

reduced visibility in this enclosure will cause additional evacuation difficulties, because people will not easily notice where the barrier on the second staircase is and are likely to collide with it glass shutter door, which is closed by a mechanical machine (mechanism), which is a prerequisite for an accident during the evacuation and may lead to an increase in the number of casualties in the building.

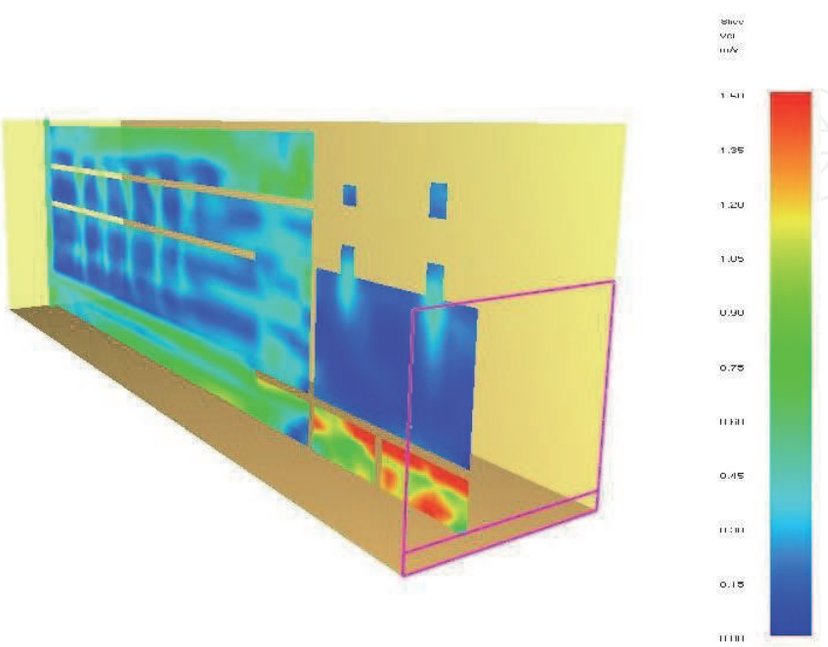

Figure 20.
Speed distribution for 3800 s of simulation.

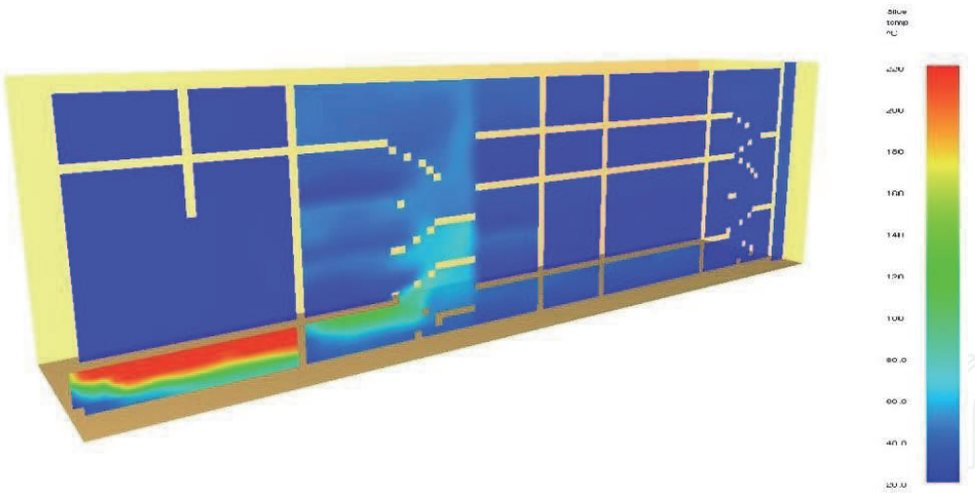

Figure 21.
Temperature distribution for the 480th second of the simulation.

Figure 20 shows the velocity distribution along the vertical section of a building for 3800 s of the simulation. It is clear that the first and last floors of the building and the staircase adjacent to the burning room are affected at the beginning of the process, and then the other floors.

Figure 21 shows the temperature distribution along the vertical section of a building for the 480th second of the simulation. From here, it is reported that in the fire zone in the laboratory the temperature is above 200°C, and at the site in the hallway in front of it, where the nearby staircase is, the temperature is above 120°C. As the building climbs, the temperature drops to about 60°C until the third floor, indicating that there should be no escape route in this area without protective clothing. By linking the data from the previous figures, the instructions for the mandatory availability of respiratory protection may also be added, as this is also the main route for the distribution of flue gases.

The results of the simulation of a fire occurring in a particular building give preliminary information about the flaws in its design with respect to fire safety. If taken into account, placing barriers in the right places, as well as revising the evacuation route from the building would lead to increased security in the event of a disaster or accident and to removal all people without damage to their health.

5. Conclusion

The results obtained in this chapter are first and foremost a practical application that allows solving problems related to fire prevention and analysis in a restricted area.

The technical solution to limit the spread of fires is to use protective water curtains, as they isolate burning vehicles from the environment and thus prevent the transfer of fire to other vehicles in the underground garage. The solution can be applied to any particular similar object.

The results of the two simulations of fire in specific buildings indicate the possibility of Fluent and FDS-PyroSim software in analyzing fire spread, smoke, temperature, and harmfulness in confined spaces. As shown, these simulations can be used:

- in the case of designing buildings with fixed sprinklers and evacuation routes.

- in judicial analysis of the consequences of the fire by initiation of its development over time.

IntechOpen

Author details

Ivan Antonov, Rositsa Velichkova*, Svetlin Antonov and Kamen Grozdanov
Technical Univesity of Sofia, Sofia, Bulgaria

*Address all correspondence to: rositsavelichkova@abv.bg

References

[1] Puzach SV, Chumachenko AP, Kozlov YI, Bubnov VM, Rodin BC. Method of calculation with a computer program for determining the actual limits of fire resistance and modeling of actions of fire extinguishing systems. In: Mechanical Ventilation and Smoke Removal During Fires. Moscow: VDPO; 2004

[2] PyroSim Example Guide. 2012. Available from: https://www.thunderheadeng.com/pyrosim/tutorials/

[3] Antonov I, Velichkova R, Grozdanov K, Uzunova M. The possibility of replacing solid walls with water curtain applicable to a large underground garage. In: EFEA'2016, Belgrade, Serbia. 2016. DOI: 10.1109/EFEA.2016.7748805. Available from: http://ieeexplore.ieee.org/document/774880/; electronic ISBN: 978-1-5090-0749-3

[4] Antonov IS. About a modification of k-ε model applicable to heat and mass transfer processes in two-phase turbulent flows. In: EMF'98 Science Conference Energy Efficiency and Environmental Protection. September 17–20, 1998, Sozopol, Proceedings. 1998. pp. 7-14

[5] CFD modeling of a large complex fire. Report 3120. Lund; 2000

[6] Drysdale D. An Introduction to Fire Dynamics. UK: Wiley; 2011

[7] Stoyanov V, Terziev A, Uzunova M. Numerical study of distribution of smoke and hazards in underground parking areas considering the operation of ventilation. In: 2014 3rd International Symposium on Environmental Friendly Energies and Applications (EFEA); St. Ouen. 2014. pp. 1-6

[8] Terziev A. Study of the fire dynamics in a burning car and analysis of the possibilities for transfer of fire to a nearby vehicle. In: 8th International Conference on Thermal Equipment, Renewable Energy and Rural Development. E3S Web of Conferences TE-RE-RD 2019; Targoviste; Romania; 6 June 2019 through 8 June 2019; Vol. 112. 2019. Article number 01015; Code 151155

[9] Antonov I. Applied Fluid Mechanics. Sofia: Technical University of Sofia; 2016

[10] Marshall AM, di Marzo M. Modeling aspects of sprinkler spray dynamics in fires. Process Safety and Environmental Protection. 2004;**82**(2):97-104

[11] Launder BE, Spalding DB. Lectures on Mathematical Models of Turbulence. London: Academic Press; 1972

[12] Leonard A. Energy cascade in large-eddy simulation of turbulent fluid flows. Advances in Geophysics. 1975;**18** (Part A):237-248

[13] Rodi W, Spalding DB. A two-parameter model of turbulence and its application to free jets. Warms and Stoffuberrtrag. 1970;**3**:585-595

[14] Abramovich GN. Theory of Turbulent Jets. Moscow; 2011. ISBN: 978-5-4365-0031-

[15] Velichkova R, Antonov I, Nikolov K, Grozdanov K, Uzunova M. Modeling of the occurrence of fire in closed cars garages. In: EFEA' 2016. DOI: 10.1109/EFEA.2016.7748807. Available from: http://ieeexplore.ieee.org/document/7748807/. Electronic ISBN: 978-1-5090-0749-3

[16] Pichurov G, Stankov P, Ivanov M. Radial jet predictions based on computational fluid dynamics. In: Healthy Buildings 2006: Creating a Healthy Indoor Environment for People, Proceedings, Vol. 5. 2006. pp. 125-128. ISBN: 978-1-62276-998-8

[17] Antonov SV, Antonov IV, Grozdanov K. Modelling and Simulation of Fire. Sofia: Technical University of Sofia; 2018

[18] Antonov I, Terziev A. Tutorial on Applied Fluid Mechanics. Sofia: Technical University of Sofia; 2012

[19] Fluent Inc. Chapter 10. Modeling turbulence. UK: Fluent; 2001

[20] Grozdanov K. TS. Modeling of fire in auto accident with the purpose of event identification [PhD thesis]. Sofia; 2017

[21] FDS-SMV Official Website. Ford Dynamics Simulator and Smokeview. Available from: https://pages.nist.gov/fds-smv/

[22] Puzach SV. Mathematical Modeling of Gas Dynamics and Heat and Mass Transfer in Solving Fire Safety Problems. Moscow: Russian Academy of Medical Science; 2003